

Magdalena Chottová Dvoráková · Uwe Pfeil ·
Jitka Kuncová · Jitka Švíglerová · Giovanni Galvis ·
Gabriela Krasteva · Peter König · Veronika Grau ·
Jana Slavíková · Wolfgang Kummer

Down-regulation of vasoactive intestinal peptide and altered expression of its receptors in rat diabetic cardiomyopathy

Received: 23 December 2004 / Accepted: 3 May 2005 / Published online: 13 December 2005
© Springer-Verlag 2005

Abstract Vasoactive intestinal peptide (VIP) is a vaso-relaxant peptide that addresses two receptor subtypes, VPAC1 and VPAC2. It stimulates insulin secretion and mediates anti-inflammatory effects and has been proposed for treatment of type 2 and autoimmune diabetes. In the heart, VIP is produced and released primarily by intrinsic neurons and improves cardiac perfusion and function. Here, we investigated the involvement of this system in the events underlying development of experimentally induced diabetic cardiomyopathy. Rats received a single streptozotocin injection, and cardiac VIP content [radioimmune assay (RIA)], expression of the VIP precursors VPAC1 and VPAC2 [real-time reverse transcription-polymerase chain reaction (RT-PCR)], and VPAC1 and VPAC2 tissue distribution (immunohistochemistry) were assessed 4, 8, and 16 weeks thereafter and compared with corresponding vehicle-treated controls. Cardiac neuropathy manifests progressively during the first 4 months of diabetes at the preproVIP mRNA and VIP peptide level and is accompanied by initial down-regulation of VPAC2 at one prime target of VIP-containing axons, i.e., smooth muscle cells of coronary arterioles. VPAC1 is expressed by macrophages. After initial changes that are specific for atria and ventricles, respectively, VPAC1 and VPAC2 expression re-

turn to control levels at 16 weeks despite ongoing loss of VIP. Given the cardioprotective role of the VIP signaling system, the persistence of receptors has therapeutic implications since it is the prerequisite for trials with VPAC2 agonists.

Keywords Autonomic neuropathy · Cardiac ganglia · Cardiac innervation · Diabetes · Heart · Rat (Wistar)

Introduction

Vasoactive intestinal peptide (VIP) is a 28-amino-acid peptide generated by enzymatic cleavage from its precursor, preproVIP, and was first isolated as a vasorelaxant from porcine gut (Said and Mutt 1970; Obata et al. 1981). It stimulates insulin secretion from insulinoma cells, mouse pancreatic islets, and perfused rat pancreas (Yada et al. 1994; Bertrand et al. 1996; Straub and Sharp 1996; Filipsson et al. 1998), and receptor subtype-specific agonists have currently been designed and suggested for use in treatment of type 2 diabetes (Tsutsumi et al. 2002; Yung et al. 2003). It is also a potent anti-inflammatory factor and has been proposed as a candidate for treatment of autoimmune diabetes (Delgado et al. 2002). In addition to its occurrence in the gastrointestinal tract, VIP is widely distributed and is also found in the extrinsic and intrinsic innervation of the heart (rat: Weihe et al. 1984; Slavíková 1997; Onuoha et al. 1999; Kuncová et al. 2003; Richardson et al. 2003), which is among those organs in which impairment during progression of diabetes mellitus is limiting for life quality and survival. Diabetic cardiomyopathy involves both the contractile cardiomyocytes and the sensory and autonomic innervation of the heart (Ziegler 1999). VIP can act directly on cardiomyocytes and relaxes coronary vascular smooth muscle, thereby improving cardiac perfusion (for review, see Henning and Sawmiller 2001). In addition, it promotes survival of peripheral neurons in culture and inhibits neuronal cell death after injury, thereby serving as a neuroprotective factor (Klimaschewski 1997). VIP actions are mediated through G-protein-coupled re-

M. C. Dvoráková · J. Kuncová · J. Švíglerová · J. Slavíková
Department of Physiology, Charles University Plzen,
Plzen, Czech Republic

U. Pfeil · G. Galvis · G. Krasteva · P. König · W. Kummer (✉)
Institute for Anatomy and Cell Biology
and University of Giessen Lung Centre,
Justus Liebig University,
Aulweg 123,
35385 Giessen, Germany
e-mail: wolfgang.kummer@anatomie.med.uni-giessen.de
Tel.: +49-641-9947000
Fax: +49-641-9947009

V. Grau
Department of General and Thoracic Surgery,
Laboratory of Experimental Surgery,
Justus Liebig University,
Giessen, Germany

ceptors that also recognize pituitary adenylate cyclase-activating peptide (PACAP) and are denoted VPAC1 and VPAC2 receptors (Harmar et al. 1998). PAC1 is a third, related receptor, that is, however, selectively activated by PACAP but not to a significant amount by VIP (Harmar et al. 1998). All three receptors are present in the rat heart (Baron et al. 2001; Sano et al. 2002), yet the cellular distribution of the individual subtypes is not known. In the present study, we investigated involvement of the endogenous VIP/VIP receptor system of the rat heart in events underlying development of diabetic cardiomyopathy in the model of streptozotocin (STZ)-induced diabetes by localizing VPAC1 and VPAC2 in the rat heart by immunohistochemistry and quantifying their expression by real-time reverse transcription-polymerase chain reaction (RT-PCR). Concomitantly, levels of VIP expression were monitored by real-time RT-PCR and radioimmunoassay (RIA). The data provide evidence for progressive reduction of endogenous VIP production in the heart during the first 4 months after onset of diabetes, with concomitant changes in the expression of receptors specific for atria and ventricles, respectively. Importantly, despite progressive loss of VIP, receptor expression returns to at least control levels after 4 months so that VPAC2 agonists that have recently been suggested as potential therapeutic tools in diabetes (Tsutsumi et al. 2002; Yung et al. 2003) may also confer cardioprotection in diabetic cardiomyopathy.

Methods

Materials and animals

STZ and other chemicals were from Sigma (St. Louis, MO, USA) or Lachema (Brno, Czech Republic) if not stated otherwise. All chemicals were of analytical grade. Adult female Wistar rats purchased from VELAZ (Prague, Czech Republic) at the age of 50 days were used for induction of diabetes and for corresponding vehicle injections. The identity of VPAC1-immunoreactive cells observed in the heart during the course of this study was investigated in another group of five adult Wistar rats obtained from Harlan Winkelmann (Borchem, Germany).

Induction of experimental diabetes

Animals at the age of 50 days were housed five per cage and fed standard laboratory chow ad libitum with free access to drinking water. All animals were left intact to adapt for 2 weeks before the initiation of the experiments. All experiments were approved by the University Committee for Experiments on Laboratory Animals and were conducted in accordance with the NIH Guide for the Care and Use of Laboratory Animals as well as the relevant guidelines of the Czech Ministry of Agriculture for scientific experimentation on animals. Diabetes was induced by a single intravenous injection of STZ (65 mg/kg body weight) dissolved in citrate buffer (pH 4.5) and verified by

severe hyperglycemia. Plasma glucose levels were measured before administration of STZ, 48 h after STZ injection, and then monthly by the glucose oxidase method (Bio-La-Test, Lachema, Czech Republic). Only animals that had glucose levels higher than 18 mmol/l were considered diabetic.

Three groups of diabetic rats, 4, 8 and 16 weeks after the onset of the disease (STZ4, STZ8, STZ16), were studied. Control, age-matched animals received a corresponding volume of vehicle and were also sacrificed by decapitation 4, 8 and 16 weeks after the injection (Contr4, Contr8, Contr16) to serve as corresponding controls.

Isolation of peritoneal macrophages

The animals were decapitated, and 100–150 ml HEPES buffer (in mM: NaCl 150, KCl 5.6, HEPES 10, NaOH 1.5, MgCl₂ 1, CaCl₂ 2, glucose 10; pH 7.4) was injected into the peritoneal cavity. The abdomen was massaged for 2 min, opened, and 100 ml of the buffer was aspirated and centrifuged at 200 g for 10 min. The pellet was resuspended in HEPES buffer and was either used for subsequent RT-PCR analysis, or cells were plated on cover-slips for subsequent immunofluorescence.

RT-PCR

Total RNA was isolated from the left and right atrium and left and right ventricle of STZ-treated and control animals ($n=5$ per group) using RNAzol B (WAK-Chemie; Bad-Soden, Germany). Contaminating DNA was destroyed with 1 U DNase/ μ g total RNA (Gibco-BRL; Karlsruhe, Germany). The RNA was reverse transcribed using Superscript RNase H⁻ Reverse Transcriptase (200 U/onset; Gibco-BRL) for 50 min at 42°C. Real-time quantitative PCR was done in the I-Cycler (Bio-Rad; Munich, Germany) using primers and QuantiTec SYBR Green PCR kit (Qiagen; Hilden, Germany). Primers were designed to amplify the sequence corresponding to nucleotides 1271–1420 (forward: GCTCAACTTCCAACCTGGAG, reverse: TTTCAGCAAAGGAAGCCAAT) of the published rat preproVIP cDNA sequence (Genbank Accession No. XM_217838), to nucleotides 915–1104 (forward: GCTGGACACCATCATCAA, reverse: TGAGCAGAAGCGTGGACTT) of the published VPAC1 cDNA (Genbank Accession No. M86835), to nucleotides 1099–1288 (forward: CACACTGCTGCTAATCCCACT, reverse: GCCTCTCCACCTTCTTTTCAG) of the published VPAC2 cDNA (Genbank Accession No. U09631), and to nucleotides 131–361 (forward: ATGGTGGGTATGGGTCA GAA, reverse: GGGTCATCTTTTCACGGTTG) of the published β -actin cDNA (Genbank Accession No. NM_031144). The PCR conditions were initial denaturation in one cycle of 15 min at 95°C followed by 50 cycles of 30 s at 95°C, 30 s at 58°C, and 30 s at 72°C. Although products emerged at a threshold of 30–33 cycles, a total of 50 cycles was run to reach saturation and to enable

quantitative analysis. All analyses were done in triplicate. The expression of preproVIP, VPAC1, and VPAC2 was normalized with β -actin as a housekeeping gene. The relative expression was calculated by comparison of the received C_T values. Values obtained for group STZ4 were compared with those for Cont4, those obtained for STZ8 with Cont8, and STZ16 with Cont16, respectively. The PCR products were separated by electrophoresis on a 2.0% TRIS-acetate-EDTA agarose gel, and their identity was verified by sequencing (MWG Biotech, Ebersberg, Germany). Controls run by omission of the RT step or by omission of template were negative.

Total RNA from isolated peritoneal macrophages was isolated by using the RNeasy mini kit (Qiagen, Hilden, Germany) according to the manufacturer's protocol. Prior to reverse transcription, 1 μ g of RNA was incubated with DNase (1 U DNase/preparation, Gibco-BRL) to eliminate any trace DNA contamination. The RNA was reverse transcribed using Superscript RNase H⁻ Reverse transcriptase (200 U/onset, Gibco-BRL) for 50 min at 42°C. The reverse transcriptase was inactivated by heating for 15 min at 75°C. For subsequent PCR, 2.5 μ l buffer II, 1.5–2 μ l MgCl₂ (15 mM), 0.6 μ l dNTP (10 mM each), 0.6 μ l of each primer (10 μ M, MWG Biotech, Ebersbach, Germany; sequences for VPAC1 and β -actin as given above), and 0.25 μ l AmpliTaq Gold polymerase (5 U/ μ l, all reagents from Perkin Elmer) were supplemented with H₂O to a final volume of 25 μ l. Cycling conditions were 12 min at 95°C, 40 cycles with 20 s at 95°C, 20 s at 60°C, 20 s at 72°C, and a final extension at 72°C for 7 min. Control reactions included the absence of DNA template and the absence of RT. The PCR products were separated by electrophoresis on a 1.2% TRIS-acetate-EDTA gel.

VIP radioimmunoassay

For quantitative determination of VIP-immunoreactivity levels, rats were killed by decapitation and their hearts were rapidly excised. Nine animals per group were analyzed. Tissues were rinsed with ice-cold saline and placed in ice-cold buffer containing 0.1 mmol/l EDTA, 5.0 mmol/l TRIS-HCl, pH 7.4, and 0.25 mol/l sucrose. The hearts were freed of connective tissue and fat and separated into the left atrium with the interatrial septum, right atrium, and free walls of both ventricles. Immediately after dissection, the tissues were frozen on dry ice and weighed. Then the samples were placed in 0.1 mol/l HCl containing 100 μ mol/l EDTA and 0.01% Na₂S₂O₅ 1:10 (w/v) and briefly pulverized. Test tubes with tissues were heated in a water bath at 95°C for 15 min and then cooled on ice. Content of the tubes was homogenized for 30 s using an Ultra-Turrax homogenizer. The homogenate was centrifuged at 10,000 g, 4°C, 20 min. The supernatant was neutralized with 1 mol/l TRIS-base and centrifuged again at 5,000 g, 4°C, 15 min. The clear supernatant was aspirated and stored at -70°C until RIA for VIP-immunoreactivity determinations.

VIP-immunoreactivity was assayed in tissue extracts by radioimmunoassay using a commercial kit (Phoenix Pharmaceuticals, CA, USA). The polyclonal rabbit antiserum was raised against the full-length synthetic peptide (human, rat, porcine sequence) and showed 100% cross-reactivity to VIP_{10–28}. There was no cross-reactivity to PACAP-38, and cross-reactivity to PACAP-27 was below 0.02%. Assay tubes were set up in duplicate, each containing 100 μ l of unknown sample or standard and 100 μ l of rabbit anti-VIP serum. After incubation (20 h) at 4°C, 100 μ l of tracer solution was added to each tube, and tubes were incubated for further 20 h. Bound radioactivity was separated by adding goat anti-rabbit IgG antiserum and centrifugation.

Recovery was assessed in another set of measurements ($n=7$) by addition of exogenous VIP at the time of heating in HCl. About 75% of added exogenous VIP could be detected in the final extract. Results were not corrected for recovery. Intra-assay variation did not exceed 10%.

Immunohistochemistry

Shock-frozen tissues from four hearts per experimental group were cut with a cryostat (Jung Frigocut 1900E, Leica, Bensheim, Germany); 8- μ m-thick sections were placed onto gelatinized slides and fixed for 10 min in cold acetone. Then they were covered for 1 h with blocking medium (PBS containing 0.1% bovine serum albumin, 10% normal porcine serum, and 0.5% Tween 20) followed by incubation with primary antibodies. Immunofluorescence was performed using monoclonal antibodies against VPAC1, clone AS58; and VPAC2, clone AS69, respectively (1:100, Sigma, Missouri, USA). Isotype-matched mouse IgG served as negative control. Antibodies were applied overnight at 4°C followed by washing steps (2 \times 10 min in PBS) and subsequent 1 h incubation with donkey-anti-mouse IgG conjugated to Cy3 (1:1,000, Dianova, Hamburg, Germany) followed by PBS washes. On some selected slides, additional labeling for α -smooth muscle actin (SMA) was performed to identify smooth muscle cells. In these cases, normal mouse serum was applied for 30 min after the Cy3-conjugated anti-mouse IgG has been applied, and a directly fluorescein isothiocyanate-conjugated mouse monoclonal SMA antibody (1:500, Sigma, Missouri, USA) was applied for 3.5 h. Finally, sections were coverslipped in carbonate-buffered glycerol at pH 8.6. Sections were evaluated using an epifluorescence microscope (Axioplan 2 imaging, Zeiss, Jena, Germany) equipped with appropriate filter combinations.

Single-labeling immunofluorescence revealed unidentified VPAC1-immunoreactive cells that were identified by double-labeling immunohistochemistry using monoclonal antibody ED1 (Serotec, Düsseldorf, Germany) as a marker for monocytes/macrophages (Dijkstra et al. 1985) on control heart sections. Acetone-fixed frozen sections were rinsed for 30 min in 1% H₂O₂ in PBS, preincubated for 30 min in blocking medium (PBS containing 1% bovine

serum albumin and 0.1% NaN₃), incubated overnight at 4°C with VPAC1 antibody (1:250), rinsed in PBS, and bound primary antibody was visualized using the anti-mouse EnVision Peroxidase kit (Dako Diagnostica, Hamburg, Germany) and 3,3'-diaminobenzidine, as recommended by the manufacturer. Following buffer rinses, monoclonal antibody ED1 (1:500) was applied for 2 h at room temperature, and after additional buffer washes, the sections were developed with anti-mouse/rabbit EnVision alkaline phosphatase kit (Dako), according to the manufacturer's recommendation, with Fast Blue as chromogen. Sections were coverslipped in glycergel (Dako) and evaluated with an Olympus BX51 microscope.

Coverslips with rat peritoneal macrophages were fixed for 10 min in ice-cold acetone and then subjected to single-labeling VPAC1 immunofluorescence as described above for frozen sections but using FITC-conjugated F(ab)₂ fragments of donkey anti-mouse IgG (1:200, Dianova). Then, coverslips were rinsed for 10 min in 4% buffered paraformaldehyde and exposed to either ED1 or ED2 monoclonal antibody pre-labeled with Alexa 647-conjugated monovalent goat F(ab) fragments directed against mouse IgG₁, according to the Zenon Alexa Fluor IgG₁ Labeling Kit description of the manufacturer (Molecular Probes, Eugene, OR, USA). In case of ED1 antibody, alternative labeling was also performed with Alexa 555-conjugated monovalent goat F(ab) fragments directed against mouse IgG₁ (Molecular Probes). Final dilution of ED1 and ED2 antibodies in these experiments was 1:25, and they were applied for 1 h at room temperature. Then, specimens were again fixed in buffered 4% paraformaldehyde, covered with carbonate-buffered glycerol, and evaluated by conventional epifluorescence microscopy and with a confocal laser scanning microscope (CLSM, TCS SP2 AOBS, Leica, Bensheim, Germany) using Ar 488 nm, He-Ne 543 nm, and He-Ne 633 nm laser lines.

Data analysis

Tissue concentrations of VIP immunoreactivity were expressed in nanograms per gram wet weight. Results are reported as means ± S.E.M. Statistical analysis was performed by means of ANOVA, with post hoc tests corrected for multiple comparisons by the Bonferroni's method using the BMDP statistical package (version 2.0, Statistical Solutions, USA). Statistical analysis of relative gene expression was done by the Kruskal–Wallis test followed by the Mann–Whitney test using SPSS software (SPSS software, Munich, Germany). Throughout, the results were considered significantly different when $P < 0.05$.

Results

VIP and its receptors in the control rat heart

In control rat hearts, mRNA coding for the VIP precursor, preproVIP, was detected in all heart chambers (Fig. 1)

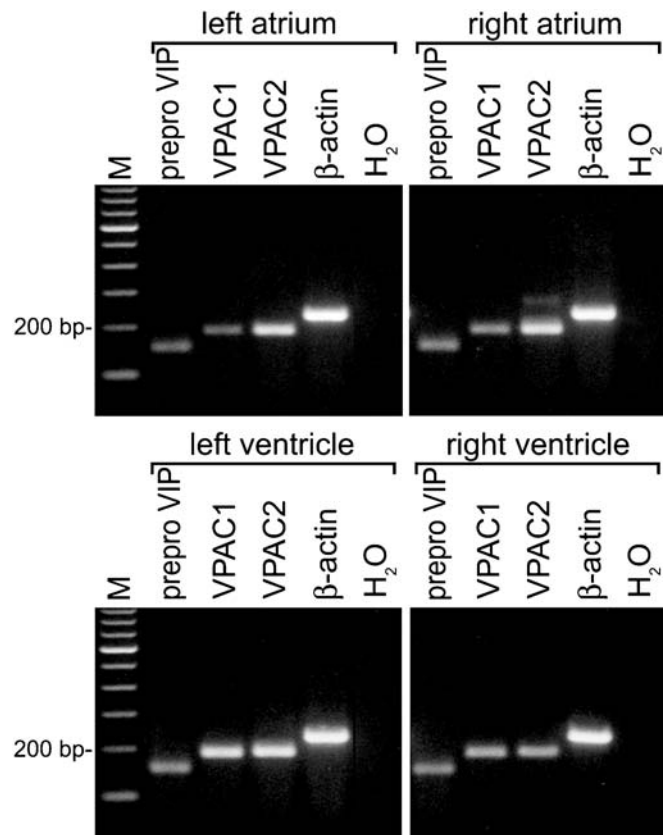


Fig. 1 Detection of mRNAs coding for preproVIP, VPAC1, and VPAC2 in rat heart compartments by qualitative reverse transcription-polymerase chain reaction (RT-PCR) and agarose gel electrophoresis. β -Actin served as housekeeping gene for standardization of quantitative RT-PCR. *M* marker, *H₂O* negative control with omission of template

although only at very low amounts in the ventricles (relative expression 6.7-fold higher in atria, as determined by quantitative RT-PCR). These expression data reflected amounts of VIP as measured by RIA, also showing markedly higher amounts in atria (Fig. 2a) than in ventricles (Fig. 2b). Messenger RNAs coding for receptor subtypes VPAC1 and VPAC2 could be detected in atria and ventricles from both sides by RT-PCR (Fig. 1). In real-time RT-PCR, Δ C_T values for VPAC1—compared with β -actin as housekeeping gene—were higher than those for VPAC2, suggesting lower expression levels of VPAC1. Similarly, immunohistochemistry using monoclonal antibodies revealed fewer VPAC1- than VPAC2-immunoreactive cells. VPAC1 immunoreactivity was restricted to small, solitary cells very infrequently found in the connective tissue spaces of all compartments of the heart (Fig. 3). These cells were often of irregular shape and exhibited granular immunolabeling. This shape and labeling pattern resembled that of macrophages, so that expression of VPAC1 by these cells was specifically investigated. Double-labeling immunohistochemistry using the monoclonal antibody ED1 as monocyte/macrophage marker showed colocalization of ED1- with VPAC1-immunoreactivity although the total number of ED1-positive cells was higher than that of

Fig. 2 Vasoactive intestinal peptide radioimmunoassay (VIP-RIA) **a** Atria: An initial trend toward elevated VIP levels (nonsignificant) is observed 4 weeks after streptozotocin (STZ) treatment, and VIP levels decrease thereafter. **b** Ventricles: A slight initial trend toward elevated VIP levels (nonsignificant) is observed 4 weeks after STZ treatment, and VIP levels decrease thereafter; * $P < 0.05$, ** $P < 0.01$ compared with 4 weeks after STZ treatment, and $P < 0.05$ compared with corresponding control group; $n = 9$ in each group

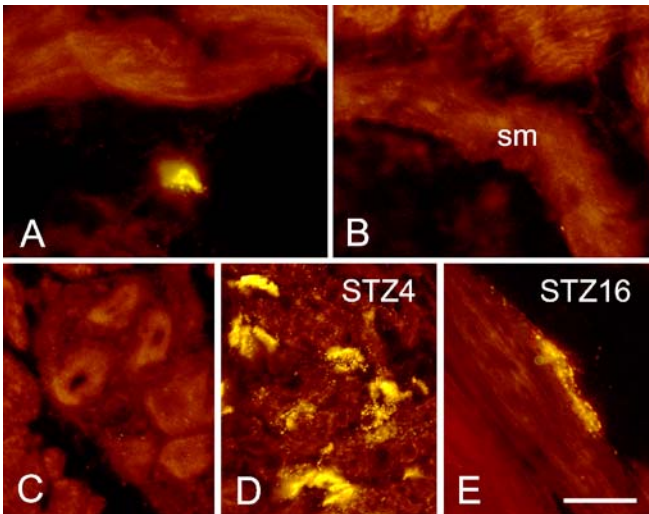
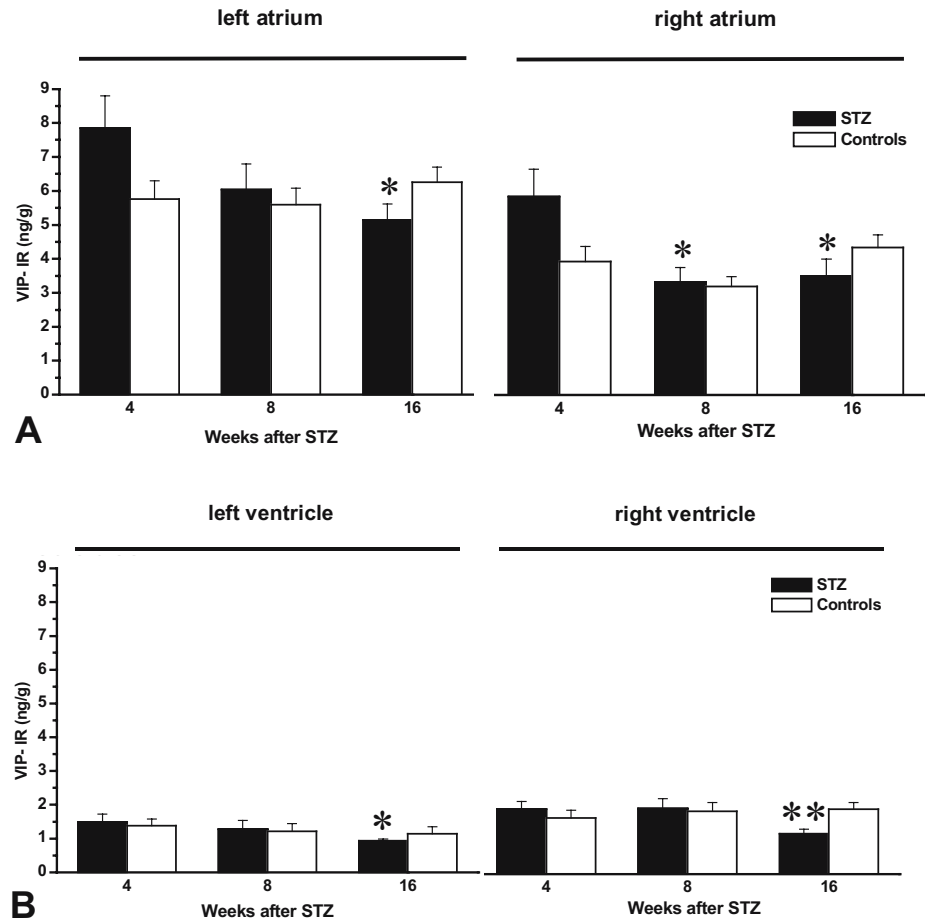


Fig. 3 VPAC1 immunolabeling in control animals was restricted to small cells with short processes exhibiting granular labeling pattern (a). Vascular smooth muscle cells (sm, b) and neurons of intrinsic ganglia (c) were negative. In diabetic animals, small VPAC1-positive cells were still observed (d) 4 weeks after onset of diabetes [streptozotocin (STZ4)] next to a local ganglion, and (e) in the epicardium 16 weeks after onset (STZ16). Bar represents 50 μ m throughout

VPAC1-immunoreactive cells (Fig. 4a). Expression of VPAC1 by macrophages was further substantiated by analysis of cells obtained by peritoneal lavage. VPAC1 mRNA was demonstrated by RT-PCR in peritoneal macrophages (Fig. 4b), and double-labeling immunofluorescence showed that the majority, although not all, of the ED1-positive peritoneal macrophages exhibited membrane-bound VPAC1 immunoreactivity (Fig. 4c). Double-labeling was also performed in combination with the monoclonal antibody ED2 that recognizes a subpopulation of differentiated macrophages. Although double-labeled (VPAC1/ED2) cells were also observed, there was, in general, an inverse correlation between VPAC1- and ED2-labeling intensities: peritoneal macrophages with the lowest VPAC1-labeling intensity showed particularly bright ED2-labeling (Fig. 4d).

On the other hand, VPAC2 immunoreactivity was found on smooth muscle cells (Fig. 5) and on single cardiomyocytes (less than 1% of total cell number; Fig. 6). Smooth muscle cells were easily identified by their characteristic morphology and their location and were additionally identified by double-labeling with a monoclonal SMA-antibody (Fig. 5d, e). VPAC2-immunoreactive smooth muscle cells included those located in the atrial endocardium and in the subendothelial layer of the entering caval and pulmonary veins, and those of small coronary branches (Fig. 5). In general, immunolabeling of ventricular arte-

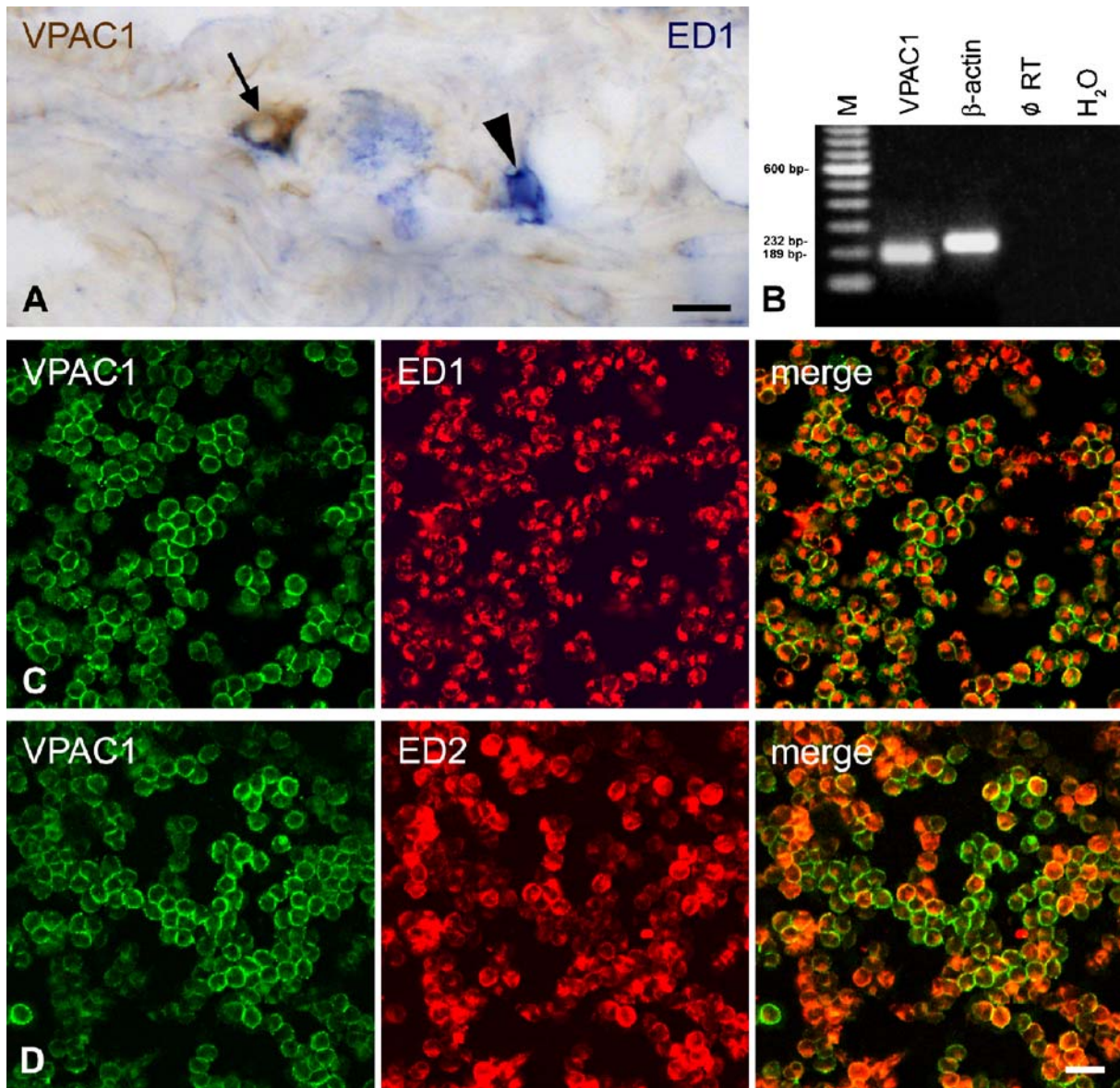


Fig. 4 VPAC1 expression in macrophages. **a** Double-labeling immunohistochemistry of frozen heart section for VPAC1 (*brown reaction product*) and ED1 (*blue*; lysosomal antigen of monocytes/macrophages) shows ED1-positive granules in a VPAC1-immunoreactive cell (*arrow*) while another ED1-positive cell is not VPAC1-immunoreactive (*arrowhead*). **b** Reverse transcriptase-polymerase chain reaction (RT-PCR) of isolated peritoneal macrophages shows VPAC1 mRNA expression. Primers specific for β -actin served as controls for RNA isolation efficacy; negative controls were run

without reverse transcription or with omission of template (H_2O). *M* marker. **c, d** Double-labeling of isolated peritoneal macrophages for VPAC1 and ED1 (**c**) or ED2 (**d**), respectively [confocal laser scanning microscope (CLSM)]. The majority of, but not all, isolated cells exhibit distinct membrane-bound VPAC1-immunolabeling. All VPAC1-immunoreactive cells are labeled by the ED1-antibody (**c, merge**). VPAC1- and ED2-labeling intensities generally show an inverse correlation although clearly double-labeled cells are also visible (**d, merge**). Bars represent 10 μm in *A* and 20 μm in *C* and *D*

rioles was not as intense as that of atrial arterioles. Small arteries and arterioles of surrounding tissues, e.g., epicardial and mediastinal fat pads, exhibited distinct VPAC2 immunoreactivity while smooth muscle cells of the large vessels arising from the heart-ascending aorta (Fig. 5b), pulmonary trunk, remained unlabeled. Occasionally, single ventricular cardiomyocytes displayed VPAC2-immunoreactivity while the majority of cardiomyocytes remained unstained in immunohistochemistry (Figs. 5, 6a). Intrinsic neurons of cardiac ganglia and nerve fibers were not labeled by the VPAC2 antibody (Fig. 5c).

Atrial alterations in STZ-induced diabetes

Significant changes in preproVIP, VPAC1, and VPAC2 expression occurred during a time course of up to 16 weeks after induction of diabetes by STZ. Distinct differences in reaction patterns were noted between atria and ventricles while right and left atria and right and left ventricles, respectively, responded in the same way. In atria, an initial trend toward elevated levels of preproVIP mRNA (Fig. 7a) and VIP (Fig. 2a) was noted at 4 weeks after onset of diabetes; however, statistical significance was not reached

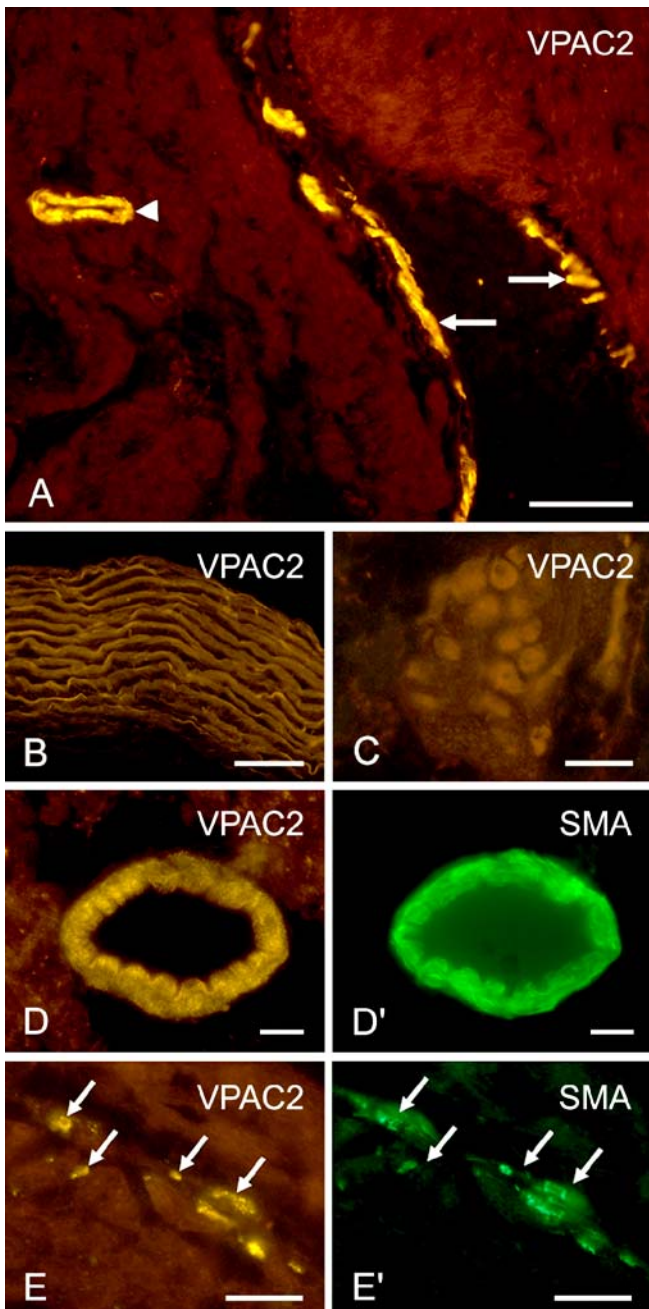


Fig. 5 VPAC2-immunolabeling in control animals was observed on the atrial subendocardial cells (**a**, arrows) and coronary arteries (**a**, arrowhead) but not on the smooth muscle cells of the aorta (**b**) and intrinsic neurons (**c**). The elastic lamellae of the ascending aorta exhibit autofluorescence (**b**). Double-labeling with a monoclonal antibody against α -smooth muscle actin (SMA) reveals VPAC2 immunoreactivity in smooth muscle cells of the coronary arteries (**d**, **d'**) and in the subendocardial layer (**e**, **e'**, arrows). Bars represent 100 μ m in **a**, 50 μ m in **b**, **c**, and 20 μ m in **d** and **e**

(e.g., $P=0.07$ for VIP in right the atrium and $P=0.10$ for VIP in the left atrium). Thereafter, however, preproVIP mRNA expression, measured by real-time RT-PCR, markedly decreased, reaching 45% of control level in the left and only 10% of control level in the right atrium 16 weeks after onset of diabetes (Fig. 7a). Similarly, VIP content of both

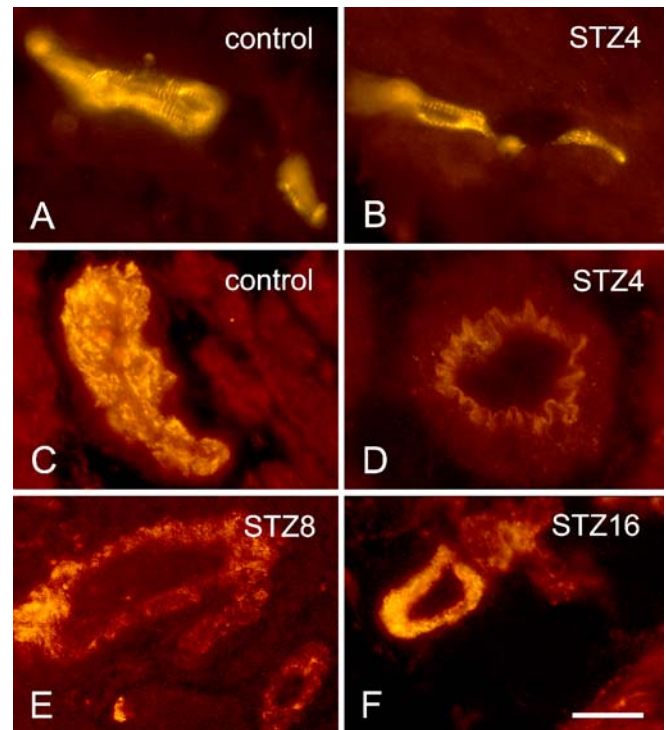


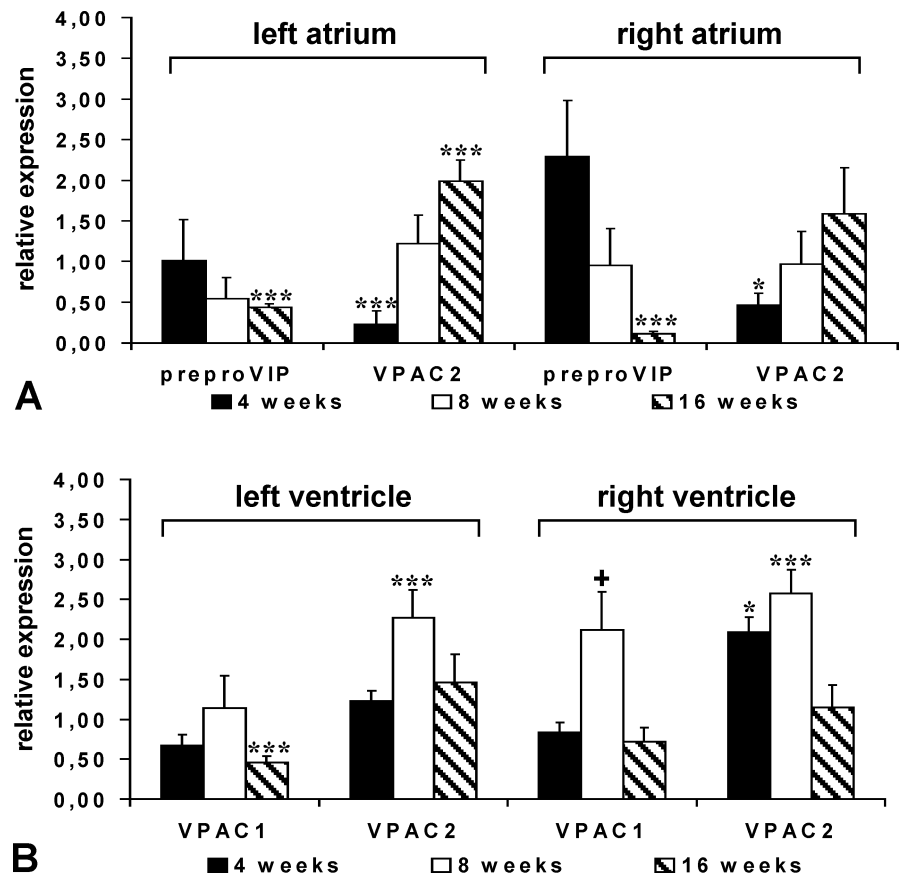
Fig. 6 VPAC2-immunofluorescence in the course of experimentally induced diabetes. Individual cardiomyocytes exhibit VPAC2-immunolabeling in control (**a**) and diabetic (**b**) animals 4 weeks after streptozotocin (STZ) treatment (STZ4). Intense immunostaining of coronary smooth muscle cells seen in controls (**c**) disappeared 4 weeks after STZ treatment (**d**), partially recovered after 8 weeks of diabetes (**e**), and was clearly visible after 16 weeks (**f**). Bar represents 50 μ m throughout

atria, measured by RIA, fell significantly in that period (Fig. 2a), although not to such an extent as that observed at mRNA levels. Conversely to the changes observed for preproVIP mRNA and VIP, VPAC2 mRNA dropped significantly to 23% (left atrium) and 58% (right atrium), respectively, at 4 weeks of diabetes, returned to initial values at 8 weeks, and reached slightly elevated levels thereafter (this increase being significant in the left atrium only) (Fig. 7a). These changes in expression pattern were paralleled by the immunohistochemical observation that VPAC2 immunoreactivity in atrial vascular and endocardial smooth muscle fully disappeared at 4 weeks of diabetes and then gradually recovered during the next 2 months (Fig. 6). Still then, however, it appeared as if labeling was not as intense and widespread as in controls. VPAC1 mRNA was qualitatively detected by RT-PCR in all experimental conditions in at least one of the atria but at such low amounts that reliable quantification was not feasible. In VPAC1 immunohistochemistry, no obvious changes compared with controls were noted (Fig. 3).

Ventricular alterations in STZ-induced diabetes

In the ventricles, an initial trend of an increase in VIP levels and then a significant drop between weeks 4 and 16 was

Fig. 7 Real-time reverse transcriptase-polymerase chain reaction (RT-PCR) quantification of preproVIP and VPAC2 mRNAs in atria (a) and ventricles (b) at 4, 8, and 16 weeks after onset of diabetes. Data for each time point are expressed in relation to the expression in the corresponding vehicle-treated group, which is set as relative expression=1. * $P<0.05$, *** $P<0.001$ (Mann–Whitney test) compared with the corresponding control group. ⁺ $P<0.05$ (Mann–Whitney test) compared with 16 weeks of diabetes; $n=5$ in each group



observed (Fig. 2b). These changes paralleled those seen in atria although the total amount of VIP in ventricles was much lower. PreproVIP mRNA was qualitatively detected by RT-PCR in all experimental conditions but at such low amounts (Δ_{CT} values higher than 12) that reliable quantification was not feasible. The time course of receptor expression in ventricles differed markedly from that seen in atria. Instead of an initial drop, elevated VPAC2 mRNA levels were observed at 4 weeks, and expression reached a significant peak at 8 weeks of diabetes to return to control levels at 16 weeks. A peak expression at 8 weeks was also observed for VPAC1 mRNA although it reached significance only in the right ventricle. There were no elevated levels before and after this peak (Fig. 7b). In immunohistochemistry, the absence of VPAC2-positive vascular smooth muscle cells in the initial stages as observed in the atria was also noted for the ventricles, but singular VPAC2-immunoreactive cardiomyocytes were present throughout (Fig. 6b). VPAC1 immunohistochemistry revealed no obvious changes compared with controls (Fig. 3).

Discussion

The present study demonstrates significant changes in the expression of the cardioprotective peptide VIP and its receptors VPAC1 and VPAC2 in the rat heart during the first 4 months of STZ-induced diabetes. Previous studies have

so far focused upon other organs and evaluated primarily VIP content by RIA and immunohistochemistry while quantitative data on the expression of preproVIP and its receptors have not yet been available. VIP is produced and secreted by many different cell types, the most prominent being endocrine cells of the gastroenteropancreatic system and various subsets of neurons (Said 1986). The effect of diabetes on VIP is clearly organ and tissue specific, and while distinct changes in both directions have been reported for several systems—e.g., retina (Troger et al. 2001), enteric nervous system (Belai et al. 1993, 1996; Nowak et al. 1995), and pancreatic endocrine cells (Adeghate et al. 2001)—others, such as sensory neurons, keep VIP content unaltered in response to STZ-induced diabetes (Steers et al. 1994; Zochodne et al. 2001; Regalia et al. 2002).

In the rat heart, VIP is primarily produced and located in a subset of neurons of atrial cardiac ganglia that project predominantly to targets in the atria, e.g., blood vessels and elements of the conducting system (Weihe et al. 1984; Slavíková 1997; Kuncová et al. 2003). Accordingly, both preproVIP mRNA and VIP levels were higher in atria than in ventricles. The present data clearly demonstrate that this part of the cardiac innervation is affected early in STZ-induced diabetes. This effect was most pronounced when analyzed at the mRNA expression level while VIP content was not reduced to a similarly high extent at 8 weeks of diabetes. This observation is best explained by a combination of severely reduced expression and additional im-

paired release of VIP from nerve terminals. Impaired release of VIP in response to electrical-field stimulation has indeed been reported for enteric neurons 8 weeks after onset of diabetes, despite detection of high amounts of VIP within nerve fibers by immunohistochemistry (Belai et al. 1987, 1996). Preliminary data from our laboratory demonstrate a further progression of the decline in VIP content during the next 8 months of diabetes (own unpublished data), showing that the alterations observed during the first 4 months are not spontaneously reversible but are, rather, pronounced in the course of the disease.

Among the VIP receptors, VPAC2 was the predominant type both at mRNA (RT-PCR) and protein levels (immunohistochemistry) in the rat heart in our study, in line with previous RT-PCR observations on the rat heart and cardiac cell cultures (Baron et al. 2001; Sano et al. 2002; DeHaven and Cuevas 2002). The use of monoclonal antibodies and immunohistochemistry allowed us to identify the cellular distribution of the receptor subtypes *in situ*, thereby showing a complementary distribution of VPAC1 and VPAC2 in the rat heart. VPAC1 immunoreactivity was restricted to macrophages in the connective tissue spaces, and these data were supported by RT-PCR and immunohistochemistry on rat peritoneal macrophages. Accordingly, VPAC1 mRNA expression has previously been reported in human resting monocytes and macrophages of different sources where VIP mediates anti-inflammatory effects (reviewed in Delgado et al. 2002, 2004). The immunohistochemically observed distribution of VPAC2, on the other hand, receives support also from RT-PCR findings obtained at isolated rat vascular smooth muscle cells (Miyata et al. 1998) and cardiomyocytes (Baron et al. 2001; Sano et al. 2002) and suggests involvement of this receptor in muscular effects, e.g., coronary vasodilatation and positive inotropism, conferred by VIP in the rat heart (for review, see Henning and Sawmiller 2001). In view of the generally low expression levels of these receptors that allow detection in the rat heart usually not by Northern blotting but only with more sensitive techniques, such as RNase protection assay or RT-PCR (Ishihara et al. 1992; Inagaki et al. 1994; Wei and Mojsov 1996; Baron et al. 2001), it might well be that additional cell types in the rat heart carry VPAC1 or VPAC2 at levels too low to be detected by immunohistochemistry.

While the diabetes-associated changes in VIP content and expression were principally identical in atria and ventricles, marked differences between these compartments were evident with regard to the VIP receptors. In the atria, which receive the majority of VIP-containing nerve fibers, VPAC2 expression was drastically down-regulated after 4 weeks of diabetes and undetectable by immunohistochemistry on the major target of VIP-containing nerve fibers, i.e., smooth muscle cells. The mechanisms underlying this down-regulation have not been addressed in the present study; however, it is striking that it was paralleled by a marked trend toward an increased VIP synthesis at this initial time point. It is conceivable that the onset of cardiac neuropathy is associated with VIP release from damaged

fibers, resulting in both compensatory increase in VIP synthesis and desensitization and down-regulation of the receptor VPAC2 (cf. McDonald et al. 1998). Consistent with this view are the observations that the initial VPAC2 down-regulation was absent in the much less densely (by VIP-containing axons) innervated ventricles and that ventricular cardiomyocytes, which are not a primary target of such axons, retained VPAC2 immunoreactivity. In the ventricles, on the other hand, VPAC1 and VPAC2 expression increased during the 2 two months of diabetes. Similarly, an increase in VPAC1 expression has been noted by semiquantitative RT-PCR in the pancreas 4 weeks after STZ treatment (Tamakawa et al. 1998). Currently, the regulatory mechanisms guiding VPAC1 and VPAC2 dynamics and expression are only partly understood (McDonald et al. 1998; Shetzline et al. 2002) and do not allow detailed interpretation of the mechanisms underlying the changes observed in diabetes. Particularly in the ventricles, which are sparsely innervated by VIP-containing axons, further understanding of the regulatory network will require also addressing non-neuronal sources of ligands for VPAC1 and VPAC2, as it is known that VIP is secreted by lymphocytes (Delgado et al. 2002) and that PACAP mRNA can be expressed, at least in culture, by rat cardiomyocytes (Sano et al. 2002).

Collectively, the data demonstrate for the first time by quantitative RT-PCR, supported by RIA and immunohistochemistry, that STZ-induced diabetes is associated with altered expression of the components of the VIP signaling system, including both the ligand and its receptors. Cardiac neuropathy manifests progressively during the first 4 months of diabetes at preproVIP mRNA and VIP peptide levels and is accompanied by initial down-regulation of VPAC2 at one prime target of VIP containing axons, i.e., smooth muscle cells of coronary arterioles. After initial changes, both VPAC1 and VPAC2 expression return to levels of control or slightly above, despite ongoing loss of VIP. This persistence of receptors has therapeutic implications since VPAC agonists have arisen as potential therapeutic tools for treatment of type 2 diabetes (Tsutsumi et al. 2002; Yung et al. 2003) and are also considered as promising candidates for treatment of autoimmune diabetes (Delgado et al. 2002). Given the protective role played by the VIP signaling system in the heart, e.g., by improving cardiac perfusion, it arises as an option that treatment with VPAC2 agonists primarily aimed at enhancing glucose-induced insulin release and glucose disposal (Tsutsumi et al. 2002) may also exert a beneficial effect on diabetic cardiomyopathy.

Acknowledgements The authors thank Ms. P. Faulhammer, Ms. P. Freitag, Ms. G. Fuchs-Moll, Ms. J. Lodrová, Ms. K. Michael, Ms. T. Papadakis, Ms. K. Pícková, and Ms. S. Wiegand for skilful technical assistance. This study was supported by the Czech Science Foundation (GACR 305/01/0263, 305/03/D180), a governmental German-Czech cooperation grant (WTZ CZE 01/014), the German Research Foundation (DFG, Research Training Groups 534 and 1062), and a Young Scientist Award of the Faculty of Medicine, Justus Liebig University.

References

- Adeghate E, Ponery AS, Pallot DJ, Singh J (2001) Distribution of vasoactive intestinal polypeptide, neuropeptide-Y and substance P and their effects on insulin secretion from the in vitro pancreas of normal and diabetic rats. *Peptides* 22:99–107
- Baron A, Monier D, Roatti A, Barettschi AJ (2001) Pituitary adenylate cyclase-activating polypeptide activates K_{ATP} current in rat atrial myocytes. *Am J Physiol Heart Circ Physiol* 280:1058–1065
- Belai A, Lincoln J, Burnstock G (1987) Lack of release of vasoactive intestinal polypeptide and calcitonin gene-related peptide during electrical stimulation of enteric nerves in streptozotocin-diabetic rats. *Gastroenterology* 93:1034–1040
- Belai A, Facer P, Bishop A, Polak JM, Burnstock G (1993) Effect of streptozotocin-diabetes on the level of VIP and mRNA in myenteric neurones. *Neuroreport* 4:291–294
- Belai A, Calcutt NA, Carrington AL, Diemel LT, Tomlinson DR, Burnstock G (1996) Enteric neuropeptides in streptozotocin-diabetic rats; effects of insulin and aldose reductase inhibition. *J Auton Nerv Syst* 8:163–169
- Bertrand G, Puech R, Maisonnasse Y, Bockaert J, Loubatieres-Mariani MM (1996) Comparative effects of PACAP and VIP on pancreatic endocrine secretions and vascular resistance in rat. *Br J Pharmacol* 117:764–770
- DeHaven WI, Cuevas J (2002) Heterogeneity of pituitary adenylate cyclase-activating polypeptide and vasoactive intestinal polypeptide receptors in rat intrinsic cardiac neurons. *Neurosci Lett* 238:45–49
- Delgado M, Abad C, Martinez C, Juarranz MG, Arranz A, Gomariz RP, Leceta J (2002) Vasoactive intestinal peptide in the immune system: potential therapeutic role in inflammatory and autoimmune disease. *J Mol Med* 80:16–24
- Delgado M, Pozo D, Ganea D (2004) The significance of vasoactive intestinal peptide in immunomodulation. *Pharmacol Rev* 56:249–290
- Dijkstra CD, Döpp EA, Joling P, Kraal G (1985) The heterogeneity of mononuclear phagocytes in lymphoid organs: distinct macrophage subpopulations in the rat recognized by monoclonal antibodies ED1, ED2 and ED3. *Immunology* 54:589–599
- Filipsson K, Sundler F, Hannibal J, Ahren B (1998) PACAP and PACAP receptors in insulin producing tissues: localization and effects. *Regul Pept* 74:167–175
- Harmar AJ, Arimura A, Gozes I, Journot L, Laburthe M, Pisegna JR, Rawlings SR, Robberecht P, Said SI, Sreedharan SP, Wank SA, Waschek JA (1998) International Union of Pharmacology. XVIII. Nomenclature of receptors for vasoactive intestinal peptide and pituitary adenylate cyclase-activating polypeptide. *Pharmacol Rev* 50:265–269
- Henning RJ, Sawmiller DR (2001) Vasoactive intestinal peptide: cardiovascular effects. *Cardiovasc Res* 49:27–37
- Inagaki N, Yoshida H, Mizuta M, Mizuno N, Fujii Y, Gono T, Miyazaki J, Seino S (1994) Cloning and functional characterization of a third pituitary adenylate cyclase-activating polypeptide receptor subtype expressed in insulin-secreting cells. *Proc Natl Acad Sci U S A* 91:2679–2683
- Ishihara T, Shigemoto R, Mori K, Takahashi K, Nagata S (1992) Functional expression and tissue distribution of a novel receptor for vasoactive intestinal polypeptide. *Neuron* 8:811–819
- Klimaschewski L (1997) VIP—a “very important peptide” in the sympathetic nervous system? *Anat Embryol* 196:269–277
- Kuncová J, Slavíková J, Reischig J (2003) Distribution of vasoactive intestinal polypeptide in the rat heart: effect of guanethidine and capsaicin. *Ann Anat* 185:153–161
- McDonald TP, Dinnis DM, Morrison CF, Harmar AJ (1998) Desensitization of the human vasoactive intestinal peptide receptor (hVIP2/PACAP R): evidence for agonist-induced receptor. *Ann NY Acad Sci* 865:64–72
- Miyata A, Sato K, Hino J, Tamakawa H, Matsuo H, Kangawa K (1998) Rat aortic smooth-muscle cell proliferation is bidirectionally regulated in a cell cycle-dependent manner via PACAP/VIP type 2 receptor. *Ann NY Acad Sci* 865:73–81
- Nowak TV, Chey WW, Chang TM, Weisbruch JP, Fouquet G (1995) Effect of streptozotocin-induced diabetes mellitus on release of vasoactive intestinal polypeptide from rodent small intestine. *Dig Dis Sci* 40:828–836
- Obata K, Itoh N, Okamoto H, Yanaihara C, Yanaihara N, Suzuki T (1981) Identification and processing of biosynthetic precursors to vasoactive intestinal polypeptide in human neuroblastoma cells. *FEBS Lett* 136:123–126
- Onuoha GN, Alpar EK, Chukwulobelu R, Nicholls DP (1999) Distributions of VIP, substance P, neurokinin A and neurotensin in rat heart: an immunocytochemical study. *Neuropeptides* 33:19–25
- Regalia J, Cai F, Helke C (2002) Streptozotocin-induced diabetes and the neurochemistry of vagal afferent neurons. *Brain Res* 938:7–14
- Richardson RJ, Grkovic I, Anderson CR (2003) Immunohistochemical analysis of intracardiac ganglia of the rat heart. *Cell Tissue Res* 314:337–350
- Said SI (1986) Vasoactive intestinal peptide. *J Endocrinol Invest* 9:191–200
- Said SI, Mutt V (1970) Polypeptide with broad biological activity: isolation from small intestine. *Science* 169:1217–1218
- Sano H, Miyata A, Horio T, Nishikimi T, Matsuo H, Kangawa K (2002) The effect of pituitary adenylate cyclase activating polypeptide on cultured rat cardiocytes as a cardioprotective factor. *Regul Pept* 109:107–113
- Shetzline MA, Walkers JKL, Valenzano KJ, Premont RT (2002) Vasoactive intestinal polypeptide type-1 receptor regulation. *J Biol Chem* 277:25519–25526
- Slavíková J (1997) Distribution of peptide-containing neurons in the developing rat right atrium, studied using immunofluorescence and confocal laser scanning. *Neurochem Res* 22:1013–1021
- Steers WD, Mackway-Gerardi AM, Ciambotti J, de Groat WC (1994) Alterations in neural pathways to the urinary bladder of the rat in response to streptozotocin-induced diabetes. *J Auton Nerv Syst* 47:83–94
- Straub SG, Sharp GW (1996) A wortmannin-sensitive signal transduction pathway is involved in the stimulation of insulin release by vasoactive intestinal polypeptide and pituitary adenylate cyclase-activating polypeptide. *J Biol Chem* 271:1660–1668
- Tamakawa H, Miyata A, Satoh K, Miyake Y, Matsuo H, Arimura A, Kangawa K (1998) The augmentation of pituitary adenylate cyclase-activating polypeptide (PACAP) in streptozotocin-induced diabetic rats. *Peptides* 19:1497–1502
- Troger J, Neyer S, Heufler C, Huemer H, Schmid E, Griesser U, Kralinger M, Kremser B, Baldissere I, Kieselbach G (2001) Substance P and vasoactive intestinal polypeptide in the streptozotocin-induced diabetic rat retina. *Investig Ophthalmol Vis Sci* 42:1045–1050
- Tsutsumi M, Claus TH, Liang Y, Li Y, Yang L, Zhu J, Dela Cruz F, Peng X, Chen H, Yung SL, Hamren S, Livingston JN, Pan CQ (2002) A potent and highly selective VPAC2 agonist enhances glucose-induced insulin release and glucose disposal. A potential therapy for type 2 diabetes. *Diabetes* 51:1453–1460
- Wei Y, Mojsov S (1996) Tissue specific expression of different human receptor types for pituitary adenylate cyclase activating polypeptide and vasoactive intestinal polypeptide: implications for their role in human physiology. *J Neuroendocrinol* 8:811–817
- Weihe E, Reinecke M, Forssmann WG (1984) Distribution of vasoactive intestinal polypeptide-like immunoreactivity in the mammalian heart. Interrelation with neurotensin- and substance P-like immunoreactive nerves. *Cell Tissue Res* 236:527–540

- Yada T, Sakurada M, Ihida K, Nakata M, Murata F, Arimura A, Kikuchi M (1994) Pituitary adenylate cyclase activating polypeptide is an extraordinarily potent intra-pancreatic regulator of insulin secretion from islet beta-cells. *J Biol Chem* 269:1290–1293
- Yung SL, Dela Cruz F, Hamren S, Zhu J, Tsutsumi M, Bloom JW, Caudle M, Rocznik S, Todd T, Lemoine L, MacDougall M, Shanafelt AB, Pan CQ (2003) Generation of highly selective VPAC2 receptor agonists by high throughput mutagenesis of vasoactive intestinal peptide and pituitary adenylate cyclase-activating peptide. *J Biol Chem* 278:10273–10281
- Ziegler D (1999) Cardiovascular autonomic neuropathy: clinical manifestations and measurements. *Diabetes Rev* 7:342–357
- Zochodne DW, Verge VM, Cheng C, Sun H, Johnston J (2001) Does diabetes target ganglion neurones? Progressive sensory neurone involvement in long-term experimental diabetes. *Brain* 124:2319–2334